Criticality Benchmarks for COG: A New Point-Wise Monte Carlo Code

H.P. Alesso, J. Pearson, J.S. Choi

Lawrence Livermore National Laboratory, Livermore, California, United States of America

INTRODUCTION

COG is a new point-wise Monte Carlo code being developed and tested at LLNL for the Cray computer. It solves the Boltzmann equation for the transport of neutrons, photons, and (in future versions) charged particles. Techniques included in the code for modifying the random walk of particles make COG most suitable for solving deep-penetration (shielding) problems. However, its point-wise cross-sections also make it effective for a wide variety of criticality problems.

COG has some similarities to a number of other computer codes used in the shielding and criticality community. These include the Lawrence Livermore National Laboratory (LLNL) codes TART and ALICE, the Los Alamos National Laboratory code MCNP, the Oak Ridge National Laboratory codes 05R, 06R, KENO, and MORSE, the SACLAY code TRIPOLI, and the MAGI code SAM. Each code is a little different in its geometry input and its random-walk modification options.[1]

Basically, COG includes:

- Cross-section data is described by the point data included on the LLNL ENDL and EGDL libraries. The current neutron library has data from 20 MeV to thermal. Photon cross sections are available from 100 MeV to 100eV.
- To check the geometry, the user may calculate volumes and draw cross-sectional pictures.
- General fixed-source routines are available. A special option, WALK-SOURCE, will take a generated source particle and will force it to collide in one, two, or three specified regions before allowing it to start its random walk.
- Random walk modification techniques include splitting and Russian roulette at both collision sites and boundaries, path stretching, survival, scattered energy bias, forced collisions, weight control, and secondary production control.
- A summary of results for random walk events includes reaction type, boundary crossings, and energy depositions. COG also makes plots indicating the location of events in phase-space.

Validating COG consists in part of running benchmark calculations against critical experiments as well as other codes.

The objective of this paper is to present calculational results of a variety of critical benchmark experiments using COG, and to present the resulting code bias. Numerous benchmark calculations have been completed for a wide variety of critical experiments which generally involve both simple and complex physical problems. The COG results, which we report in this paper, have been excellent.

In addition, the results from COG are compared to results we calculated using several other Monte Carlo codes: MORSE-C[2] (which is an LLNL modified code based on the ORNL code MORSE[3]), KENO-IV[4], KENO-Va[5], and MCNP[6]; and the discrete ordinates code SAN which is an LLNL version of ANISN[7,8]. For these calculations, the ENDL library of neutron cross sections[2] was used with COG. A 92 group set (N92GRP) of multigroup cross sections[9] derived from the ENDL library was used with MORSE-C and SAN. The 16 group Hansen-Roach cross section set[10] and a modified set with potential scattering were used with KENO-IV. With KENO-Va, the 27, 123, and 218 group ENDF-B IV cross-sections[11,12] were used. With MCNP the code's standard cross sections based on ENDF/B-V were used[6,13]. The resulting biases calculated for these code and cross section set combinations are compared for various thermal and fast systems.

BENCHMARKS

Tables 1A and 1B present a list of the benchmark problems and some general information about each. Detailed references and the multiplication factors calculated for each case using the computer codes COG, MCNP, MORSE-C, KENO-IV, KENO-Va and SAN are shown. Each benchmark case is identified by an ID designator.

Table 1A provides a list of the critical experiments used for this benchmark. The first column is an identification designator. This ID designator connects the information supplied in Table 1A with both the information in Table 1B and the graphs in Figures 1 and 2. The second column identifies the fuel form. Next, the fuel isotope is shown followed by % of isotopic content and concentration. The sixth column shows the general fuel core configuration followed by reflector material and thickness. In column 9, the mean neutron energy in Mev is displayed. Finally, a reference number to the original critical experiment paper is listed. The appropriate reference at the end of this paper will lead the reader to greater detail of the experiment by the original experiment authors.

In Table 1B, the calculation results of the codes for each identification designator, (associated with Table 1A) are listed by k-eff and the one standard deviation value.

This study has included many different types of critical experiments for the purpose of benchmark comparisons. From a neutron energy standpoint, these included both the fast metal and the thermalized solution systems. From a fissle system standpoint, it considers Pu-239, U-235, and U-233 systems. In addition, bare and reflected systems with metal or hydrogenous reflectors were considered. The geometries of these critical experiments also spanned from simple spheres to concentric cylinders, as well as annular cylindrical tanks and nuclear reactors.

To synthesis and analyze the computer results of these diverse cases, we grouped them into categories containing some common feature. We then examined whether specific biases or trends developed with each of these computational methods.

The grouping categories we selected for fast systems (Figure 1) are: (1) Plutonium-239, (2) Uranium-235, (3) Uranium-233, (4) bare core problems, (5) problems reflected by Beryllium, and (6) problems reflected by Tungsten.

The grouping categories we selected for thermal systems (Figure 2) are: (1) water reflected, low enrichment uranium fluoride solution, (2) bare high enrichment uranium nitrate solution, (3) plutonium nitrate solution, (4) water reflected PuO_2, (5) concrete reflected, high enrichment uranium nitrate, (6) water reflected, mixed nitrate solution, and (7) reactor core. We performed fewer thermal calculations and as a result, we had less data points for our comparisons within a thermal category.

RESULTS

Figures 1 and 2 display our synthesized results for fast and thermal systems respectively. In Figure 1 the critical experiment k-eff = 1 line is drawn. The y-axis shows k-eff. On the x-axis the averaged calculational results for each code for each composite group is displayed.

For example, at the top of the graph in Figure 1, Pu-239(12) shows that we grouped 12 critical experiments that were all fast and had similar characteristics. At the bottom of the graph, the ID designator C1-C12 refers back to Tables 1A and 1B information. We computed the average k-eff for these 12 experiments along with the composite standard deviation for each. As a result, the circle at the extreme left of the graph represents the average k-eff for 12 Pu-239 fast critical experiments with the composite standard deviation error bar shown for COG. The darkened circle next to it is the composite k-eff result for MCNP. Next, the open triangle shows the Keno IV results followed by a darkened triangle for MORSE-C.

The next column on the graph in Figure 1 present the results for the four codes for 15 U-235 systems. This is followed by average values for 11 U-233 systems and so on.

Results of the fast-metal systems as calculated by these four codes are shown in Figure 1. It indicates a general agreement among the results of the four codes for the U-235, the Pu-239, and the bare systems considered. However, for the U-233 systems the MORSE-C/92 group consistently yields k-eff values 2% below critical. For metal systems reflected by beryllium and tungsten alloy, the KENO-IV/16 group consistently yields k-eff values 2.5 and 1.5% above critical, respectively. Such trends or systematic errors were not found in the point-wise Monte Carlo codes (i.e., MCNP and COG).

Results for the thermal systems shown in Figure 2 again demonstrate that the point-wise codes COG and MCNP gave good agreement with critical experiments. The group-wise code KENO-IV and MORSE-C continued to show an overall bias due to group-wise cross-sections. However, we do not have enough cases in the thermal systems examined to adequately represent a statistical sample for each of the selected categories.

Pointwise Monte Carlo methods, such as those employed by COG and MCNP, have not demonstrated a systematic bias, since the cross sections they use vary continuously with energy and inherently cover all ranges of neutron energy.

The COG results were excellent for the wide variety of thermal and fast critical problems we considered. The overall bias for COG was +0.00057, the bias for thermal systems was +0.00480, and the bias for fast systems was -0.00050. We found no abnormal trends for COG, while we found anomalous systematic trends for both KENO-IV and MORSE-C (for the cross-section sets selected). In general, we conclude that COG performed excellently and consistently.

Table 1A

List of Problems, Descriptions, and References

ID	Fuel					Reflector		MFE	Reference
	Form	Iso	Iso [wt%]	U or Pu [g/cc]	Shape	Material	Thick [cm]	[MeV]	
A1	metal	U235	93.9	18.810	sphere	None		1.1E+00	14a,15
A2	metal	U235	93.7	18.740	sphere	None		1.0E+00	14b,16
A3	metal	U235	94.6	18.750	sphere	None		1.1E+00	17a,37
A4	metal	U235	93.9	18.500	sphere	Be	4.70	8.1E-01	14c,18
A5	metal	U235	93.6	18.600	sphere	Be	11.79	5.9E-01	14d,16,18
A6	metal	U235	93.2	18.490	sphere	Be	20.27	4.7E-01	19a
A7	metal	U235	93.9	18.700	sphere	C	10.16	8.9E-01	14e,20
A8	metal	U235	93.8	18.380	sphere	Ni	4.94	9.4E-01	14f,15,18
A9	metal	U235	94.0	18.430	sphere	Cu	10.56	8.1E-01	14g,15,18
A10	metal	U235	93.9	18.750	sphere	W	5.08	8.6E-01	14h,16,18
A11	metal	U235	93.9	18.750	sphere	W	10.16	7.9E-01	14i,18
A12	metal	U235	93.9	18.700	sphere	U238	1.77	1.1E+00	14j,15,16
A13	metal	U235	94.0	18.670	sphere	U238	4.47	1.1E+00	14k,15,16
A14	metal	U235	93.9	18.690	sphere	U238	9.98	1.1E+00	14m,15,16,21
A15	metal	U235	93.2	18.620	sphere	U238	18.01	1.2E+00	14n,15,16
A16	UO2(NO3)2	U235	93.1	0.020	sphere	None		3.2E-08	22a,23,24
A17	UO2F2	U235	4.9	0.728	cylinder	H2O	20.00	3.6E-08	25,26a
A18	UO2F2	U235	4.9	0.650	cylinder	H2O	20.00	3.4E-08	25,26b
A19	UO2(NO3)2	U235	93.2	0.357	annular	Concrete	20.32		36a
A20	UO2	U235	2.5	9.007	reactor				35a
B1	metal	U233	98.1	18.420	sphere	None		1.3E+00	14p,15,16
B2	metal	U233	98.2	18.620	sphere	Be	2.04	1.2E+00	14q,16,27
B3	metal	U233	98.2	18.640	sphere	Be	4.20	1.1E+00	14r,16,27
B4	metal	U233	98.2	18.620	sphere	W	2.44	1.2E+00	14s,16,27
B5	metal	U233	98.2	18.640	sphere	W	5.79	1.1E+00	14t,16,27
B6	metal	U233	98.2	18.620	sphere	U238	2.30	1.3E+00	14u,16,27
B7	metal	U233	98.2	18.640	sphere	U238	5.31	1.4E+00	14v,16,27
B8	metal	U233	98.1	18.420	sphere	U238	19.89	1.5E+00	15a,16
B9	metal	U233	98.1	18.620	sphere	U235(93.2)	1.21	1.3E+00	14w,15,27
B10	metal	U233	98.1	18.640	sphere	U235(93.2)	1.99	1.2E+00	14x,15,27
B11	metal	U233	97.9	17.780	sphere	U235(93.2)	4.82	1.1E+00	14y
B12	UO2(NO3)2	U233	98.4	0.017	sphere	None		3.2E-08	22b,23,24
C1	metal-d	Pu239	92.0	15.450	sphere	None		1.4E+00	14z,15,16,28
C2	metal-a	Pu239	94.5	19.740	sphere	H2O	20.00	1.1E+00	15b
C3	metal-d	Pu239	94.8	15.620	sphere	Be	3.69	1.2E+00	14aa,16,27
C4	metal-d	Pu239	93.7	15.800	sphere	Be	5.25	1.1E+00	16,29a
C5	metal-d	Pu239	93.7	15.800	sphere	C	3.83	1.3E+00	16,29b
C6	metal-d	Pu239	93.7	15.800	sphere	Ti	8.00	1.4E+00	16,29c
C7	metal-d	Pu239	94.8	15.620	sphere	W	4.70	1.2E+00	14bb,16,27
C8	metal-d	Pu239	94.8	15.620	sphere	U235(93.2)	1.66	1.3E+00	14cc,15,27
C9	metal-d	Pu239	93.7	15.800	sphere	U238	1.93	1.4E+00	16,29d
C10	metal-d	Pu239	94.8	15.620	sphere	U238	4.13	1.4E+00	14dd,15,16,27
C11	metal-d	Pu239	93.7	15.800	sphere	U238	6.74	1.5E+00	16,29e
C12	metal-d	Pu239	94.8	15.360	sphere	U238	19.61	1.5E+00	14ee,15,16
C13	Pu(NO3)4	Pu239	97.4	0.009	sphere	None		3.8E-08	30a
C14	Pu(NO3)4	Pu239	95.4	0.039	sphere	None		4.9E-08	32a
C15	Pu(NO3)4	Pu239	95.4	0.140	sphere	H2O	25.00	8.6E-08	31a,32
C16	Pu(NO3)4	Pu239	94.0	0.012	cylinder	H2O	15.00	3.9E-08	33a
	UO2(NO3)2	U235	0.7	0.030					
C17	PuO2	Pu239	100.0	9.960	sphere	H2O	30.48	7.3E-01	16a

Table 1B

List of Problems and Results

ID	COG k-eff	COG dk-eff	MCNP k-eff	MCNP dk-eff	MORSE-C k-eff	MORSE-C dk-eff	KENO k-eff	KENO dk-eff	KENO Version	SAN k-eff
A1	1.0002	0.0029	0.9954	0.0037	0.9990	0.0029	1.0006	0.0034	IV/16	1.0029
A2	0.9987	0.0028	1.0031	0.0033	1.0033	0.0030	1.0043	0.0036	IV/16	1.0050
A3	1.0009	0.0029			0.9997	0.0030	1.0005	0.0030	IV/16	1.0030
A4	0.9967	0.0025	1.0005	0.0035	1.0039	0.0030	1.0244	0.0034	IV/16	1.0116
A5	0.9957	0.0026	0.9935	0.0037	0.9999	0.0029	1.0296	0.0041	IV/16	0.9986
A6	0.9961	0.0037			0.9966	0.0030	1.0361	0.0038	IV/16	0.9819
A7	1.0056	0.0078	1.0265	0.0033	1.0010	0.0030	0.9871	0.0041	IV/16	1.0024
A8	0.9964	0.0027	0.9971	0.0035	1.0162	0.0030	0.9965	0.0039	IV/16	1.0143
A9	1.0084	0.0028	0.9906	0.0028	1.0186	0.0030	0.9992	0.0037	IV/16	1.0184
A10	0.9986	0.0027	1.0142	0.0036	1.0016	0.0030	1.0158	0.0037	IV/16	1.0040
A11	1.0002	0.0028	1.0074	0.0027	1.0054	0.0030	1.0119	0.0031	IV/16	1.0020
A12	0.9978	0.0028	1.0071	0.0044	1.0041	0.0030	1.0001	0.0031	IV/16	1.0066
A13	1.0012	0.0027	1.0054	0.0030	1.0135	0.0030	1.0045	0.0033	IV/16	1.0117
A14	1.0013	0.0027	1.0026	0.0028	1.0061	0.0030	1.0031	0.0038	IV/16	1.0094
A15	1.0004	0.0033	1.0073	0.0030	1.0014	0.0030	1.0022	0.0031	IV/16	1.0056
A16	0.9917	0.0045			1.0069	0.0030	1.0085	0.0104	IV/16	0.9980
A17	1.0010	0.0030	1.0033	0.0035	0.8198	0.0029	0.9950	0.0035	IV/16	
A18	1.0015	0.0064	1.0010	0.0039	0.8467	0.0029	0.9971	0.0030	IV/16	
A19	0.9935	0.0063					0.9941	0.0063	IV/16	
A20	1.0032	0.0124					0.9790	0.0038	Va/27	
							1.0008	0.0040	Va/123	
							0.9789	0.0045	Va/218	
B1	0.9952	0.0028	0.9925	0.0035	0.9801	0.0030	1.0052	0.0040	IV/16	0.9792
B2	0.9984	0.0027	0.9942	0.0033	0.9770	0.0030	1.0080	0.0044	IV/16	0.9842
B3	1.0034	0.0022	0.9925	0.0048	0.9854	0.0031	1.0199	0.0045	IV/16	0.9884
B4	0.9992	0.0027	1.0011	0.0047	0.9756	0.0031	1.0200	0.0044	IV/16	0.9800
B5	0.9926	0.0028	1.0033	0.0032	0.9679	0.0030	1.0105	0.0038	IV/16	0.9779
B6	0.9992	0.0029	0.9977	0.0034	0.9827	0.0031	0.9948	0.0039	IV/16	0.9855
B7	1.0084	0.0028	0.9975	0.0037	0.9869	0.0030	0.9962	0.0042	IV/16	0.9888
B8	0.9983	0.0027	1.0034	0.0035	0.9836	0.0030	0.9893	0.0039	IV/16	0.9879
B9	1.0078	0.0028	0.9872	0.0040	0.9854	0.0030	1.0027	0.0044	IV/16	0.9860
B10	0.9947	0.0027	1.0005	0.0038	0.9870	0.0030	1.0012	0.0048	IV/16	0.9919
B11	0.9960	0.0027	0.9991	0.0029	1.0081	0.0030	1.0061	0.0037	IV/16	1.0054
B12	0.9984	0.0027			1.0082	0.0029	1.0041	0.0085	IV/16	1.0140
C1	1.0011	0.0030	0.9951	0.0034	1.0001	0.0031	1.0001	0.5000	IV/16	1.0029
C2	1.0104	0.0088			0.9940	0.0048	0.9912	0.0038	IV/16	0.9710
C3	1.0002	0.0030	0.9907	0.0038	1.0033	0.0032	1.0121	0.0049	IV/16	1.0052
C4	0.9964	0.0030	0.9982	0.0041	0.9988	0.0032	1.0256	0.0045	IV/16	1.0039
C5	1.0055	0.0042	0.9905	0.0038	0.9996	0.0030	0.9921	0.0042	IV/16	1.0049
C6	0.9864	0.0042	0.9752	0.0043	0.9785	0.0034	0.9846	0.0044	IV/16	0.9905
C7	0.9959	0.0032	1.0068	0.0040	0.9950	0.0030	1.0100	0.0044	IV/16	0.9973
C8	1.0074	0.0028	1.0016	0.0037	1.0060	0.0030	1.0083	0.0046	IV/16	1.0038
C9	0.9947	0.0028	0.9939	0.0032	0.9944	0.0031	0.9951	0.0044	IV/16	0.9974
C10	0.9931	0.0029	0.9985	0.0051	1.0098	0.0030	1.0008	0.0039	IV/16	1.0056
C11	0.9991	0.0047	0.9909	0.0039	0.9926	0.0030	0.9930	0.0042	IV/16	1.0019
C12	0.9952	0.0032	1.0027	0.0033	1.0036	0.0030	0.9914	0.0031	IV/16	1.0028
C13	1.0164	0.0047			1.0208	0.0028	1.0191	0.0020	IV/16	1.0230
C14	1.0018	0.0030			1.0219	0.0030	1.0081	0.0029	IV/16	1.0216
							1.0300	0.0050	Va/27	
							1.0360	0.0049	Va/123	
							1.0211	0.0050	Va/218	
C15	1.0380	0.0047			1.0098	0.0049	1.0547	0.0032	IV/16	1.0170
C16	1.0042	0.0066			1.0141	0.0029	1.0233	0.0017	IV/16	
C17	1.0018	0.0153			0.9988	0.0030	1.0227	0.0055	IV/16	0.9789

Figure 1. Comparison of code Results of the Fast-Metal Systems (55)

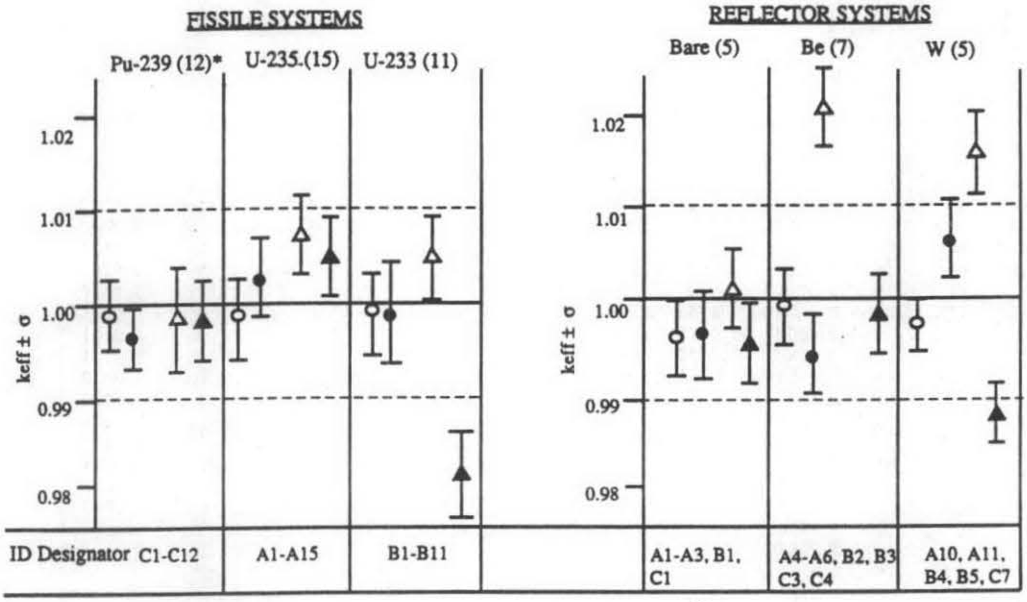

$$\bar{k}eff = \frac{\Sigma(ki/\sigma_i^2)}{\Sigma(1/\sigma_i^2)}; \quad \bar{\sigma} = \left[\sum_{i=1}^{N}\left(\frac{1}{1/\sigma_i^2}\right)\right]^{1/2}$$

Figure 2. Comparison of Code Results for Thermal Systems (11)

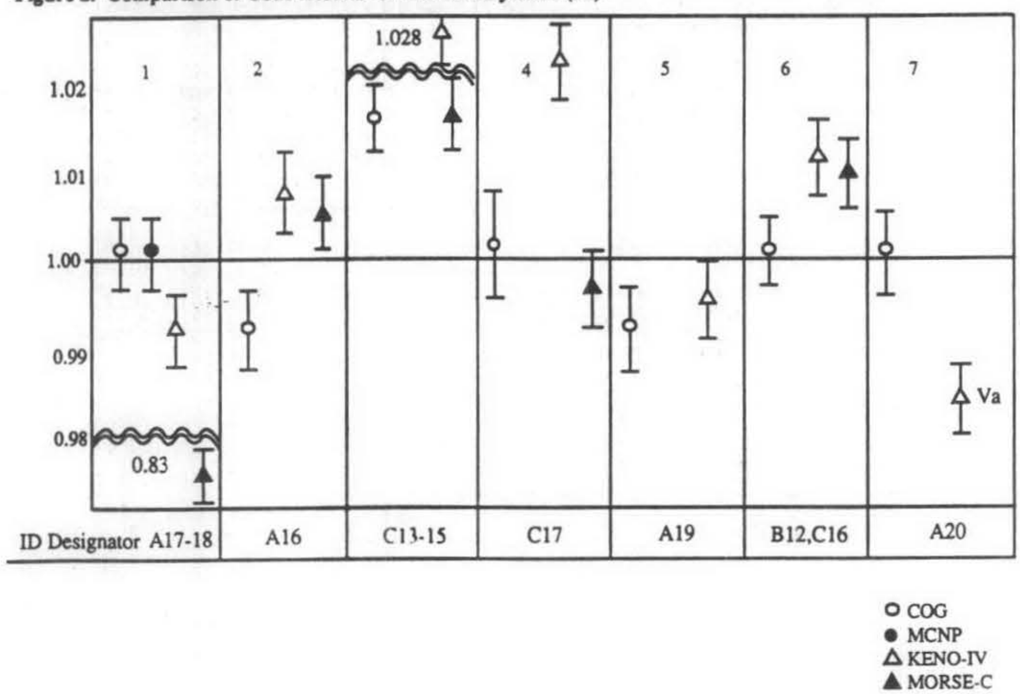

REFERENCES

1. T.P. Wilcox, Jr. and E.M. Lent, *"COG: Particle Transport Code Designed to Solve the Boltzman Equation for Deep-Penetration (Shielding) Problems,"* Lawrence Livermore National Laboratory (April 1989).

2. T.P. Wilcox, *"MORSE-C, A CDC-7600 Program Designed to Solve Nuclear Criticality Problems by Using the Monte Carlo Method,"* UCID-18993, Lawrence Livermore National Laboratory (January 30, 1981).

3. E.A. Straker, P.N. Stevens, D.C. Irving and V.R. Cain, *"The MORSE Code - A Multigroup Neutron and Gamma-Ray Monte Carlo Transport Code,"* ORNL-4585, Oak Ridge National Laboratory (September 1970).

4. L.M. Petrie and N.F. Cross, *"KENO-IV - An Improved Monte Carlo Criticality Program,"* ORNL-4938, Oak Ridge National Laboratory (November 1975).

5. L.M. Petrie and N.F. Cross, *"KENO-Va: An Improved Monte Carlo Criticality Program with Supergrouping,"* NUREG/CR-0200, ORNL/NUREG/CSD-2, Vol. 2, Sec. F11, Oak Ridge National Laboratory (November 1985).

6. J.F. Briesmeister, ed., *"MCNP - A General Monte Carlo Code for Neutron and Photon Transport,"* LA-7396-M, Rev. 2, Los Alamos National Laboratory (September 1986).

7. W.W. Engle, Jr., *"A User's Manual for ANISN: A One-Dimensional Discrete Ordinates Transport Code with Anisotropic Scattering,"* K-1693, Oak Ridge Gaseous Diffusion Plant (1967).

8. K.D. Lathrop, *"The S Method,"* Y-CDC-11, Union Carbide Corp. (1970).

9. M.A. Gardner and R.J. Howerton, *"ACTL: Evaluated Neutron Activation Cross-Section Library - Evaluation Techniques and Reaction Index,"* UCRL-50400, Vol. 18, Lawrence Livermore National Laboratory (October 1978).

10. G.E. Hansen and W.H. Roach, *"Six and Sixteen Group Cross Sections for Fast Intermediate Critical Assemblies,"* LAMS-2543, Los Alamos Scientific Laboratory (1961).

11. N.M. Greene, et al., *"AMPX: A Modular Code System for Generating Coupled Multigroup Neutron Gamma Libraries from ENDF/B,"* ORNL/TM-3706, Oak Ridge National Laboratory (1976).

12. W.E. Ford, et al., *"A 218-Group Neutron Cross-Section Library in the AMPX Master Interface Format for Criticality Safety Studies,"* ORNL/CSD/TM-4, Oak Ridge National laboratory (July 1976).

13. R. Kinzey, *"Data Formats and Procedures for the Evaluated Nuclear Data File, ENDF,"* BNL-NCS-50496 (ENDF 102) 2nd Edition (ENDF/B-V), Brookhaven National Laboratory (October 1979).

14. H.C. Paxton, *"Los Alamos Critical-Mass Data,"* LA-3067-MS, Rev., Los Alamos Scientific Laboratory (November 1975). (a) Table IA1, case 2, (b) Table IA1, case 1, (c) Table IC3, case 10, (d) Table IC3, case 12, (e) Table IC4a, case 2, (f) Table IC2, case 8, (g) Table IC2, case 4, (h) Table IC1, case 3, (i) Table IC1, case 4, (j) Table IB1, case 5, (k) Table IB1, case 4, (m) Table IB1, case 2, (n) Table IB1, case 1, (p) Table IV, case 1, (q) Table IV, case 8, (r) Table IV, case 7, (s) Table IV, case 6, (t) Table IV, case 5, (u) Table IV, case 4, (v) Table IV, case 3, (w) Table VA, case 9, (x) Table VA, case 10, (y) Table VA, case 11, (z) Table IIIA1, case 1, (aa) Table IIIA1, case 11, (bb) Table IIIA1, case 8, (cc) Table VA, case 1, (dd) Table IIIA1, case 6, (ee) Table IIIA1, case 4.

15. G.E. Hansen and H.C. Paxton, *"Reevaluated Critical Specifications of Some Los Alamos Fast-Neutron Systems,"* LA-4208, Los Alamos Scientific Laboratory, (June 1969). (a) p.9, 5.74 ± 0.03 kg U^{233}(98.13 wt%), (b) p.12, 5.79 kg ± 0.5% sphere of Pu^{239}(94.5%).

16. H.C. Paxton and N.L. Pruvost, *"Critical Dimensions of Systems containing ^{235}U, Pu^{239}, and U^{233}, 1986 Revision,"* LA-10860-MS, Los Alamos National Laboratory, (July 1987). (a) Table 16, line 3, 6.6±0.2cm sphere.

17. *"Argonne Code Center: Benchmark Problem Book,"* ANL-7416, Argonne National Laboratory, (July 16, 1968). (a) Problem 1.

18. G.E. Hansen, H.C. Paxton and D.P. Wood, *"Critical Masses of Oralloy in Thin Reflectors,"* LA-2203, Rev., Los Alamos Scientific Laboratory, (July 16, 1958).

19. H.R. Ralston, *"Critical Masses of Spherical Systems of Oralloy Reflected in Beryllium,"* UCRL-4975, University of California Radiation Laboratory, Livermore, (October 10, 1957), (a) Table I, case 1.

20. E.C. Mallary, *"Oralloy Cylindrical Shape Factor and Critical Mass Measurements in Graphite, Parafin, and Water Tampers,"* LA-1305, Los Alamos Scientific Laboratory (October 27, 1951).

21. G.E. Hansen and D.P. Wood, *"Precision Critical Mass Determinations for Oralloy and Plutonium is Spherical Tuballoy Tampers,"* LA-1356, Los Alamos Scientific Laboratory (February 1, 1952).

22. Alan Staub, D.R. Harris, and Mark Goldsmith, *"Analysis of a Set of Homogeneous U-H_2O Spheres,"* Nucl. Sci. and Eng., **34** (1968) 263-274. (a) Experiment number 1, (b) Experiment number 5.

23. R. Gwin and D.W. Magnuson, *"Critical Experiments for Reactor Physics Studies,"* ORNL-60-4-12, Oak Ridge National Laboratory (1960).

24. R. Gwinn and D.W. Magnuson, *"Determination of Eta by Comparison of $\eta\sigma$ for U^{233} and Pu^{239} with $\eta\sigma$ for U^{235} in a Flux Trap Critical Assembly,"* Nucl. Sci. & Eng., **12** (1962) 359-363.

25. S. Morioka, Y. Hariyama, H. Kadptani, M. Senda, K. Tamura and K. Saito, *"Criticality Safety Analysis with the Monte Carlo Code MCNP,"* International Seminar on Nuclear Criticality Safety, Tokyo, Japan (October, 1987) 335-339.

26. E.B. Johnson and D.F. Cronin, *"Critical Dimensions of Aqueous UO_2F_2 Solutions Containing 4.9% ^{235}U-Enriched Uranium,"* ORNL-3714, Oak Ridge National Laboratory (Dec. 1964) 31-33. (a) Table 2.2.1, case 3, (b) Table 2.2.1, case 4.

27. E.A. Plassmann and D.P. Wood, *"Critical Reflector Thicknesses for Spherical U^{233} and Pu^{239} Systems,"* Nucl. Sci. & Eng., **8** (1960) 615-620.

28. G.A. Jarvis, G.A. Linenberger, J.D. Ornfoff and H.C. Paxton, *"Two Plutonium-Metal Critical Assemblies,"* Nucl. Sci. & Eng., **8** (1960) 525-531.

29. F.A. Kloverstrom, *"Spherical and Cylindrical Plutonium Critical Masses,"* UCRL-4957, University of California Radiation Laboratory, Livermore (September 1957). (a) Table II, case 7, (b) Table II, case 3, (c) Table II, case 5, (d) Table II, case 1, (e) Table II, case 6.

30. R.C. Lloyd, R.A. Libby, and E.D. Clayton, *"The Measurement of Eta and the Limiting Concentration of the Pu^{239} in Critical Aqueous Solutions,"* Nucl. Sci. & Eng., **82** (1982) 325-331. (a) Table I, case 4.

31. C.R. Richey, *"Theoretical Analyses of Homogeneous Plutonium Critical Experiments,"* Nucl. Sci. & Eng., **31** (1968) 32-39. (a) Table III, 11.5-in. diameter, 140 gPu/1.

32. R.C. Lloyd, C.R. Richey, E.D. Clayton and D.R. Skeen, *"Critical Studies with Plutonium Solutions,"* Nucl. Sci. & Eng., **25** (1966) 165-173. (a) Table I, footnote d, H/Pu = 668.

33. R.C. Lloyd and E.D. Clayton, *"Criticality of Plutonium-Uranium Nitrate Solution Containing 30 wt% Pu,"* Trans. ANS, **17** (1973) 269-270. (a) Table I, 12.4 gPu/1 case.

34. R.C. Lloyd and E.D. Clayton, *"Effect of Fixed and Soluble Neutron Absorbers on the Criticality of Uranium-Plutonium Systems,"* Nucl. Sci. & Eng., **62** (1977) 726-735.

35. M.N. Baldwin, G.S. Hoovler, R.L. Eng and F.G. Welfare, *"Critical Experiments Supporting Close Proximity Water Storage of Power Reactor Fuel, Summary Report,"* BAW-1484-7, Babcock & Wilcox Co., Lynchburg, VA, (1979). (a) case XIIIa.

36. Robert E. Rothe, *"Criticality Safety of an Annular Tank for Fissile Solution,"* Trans. Am. Nucl. Soc., **39** (1981) 525-527. (a) Table I, configuration I, 0.8% boron-loaded concrete "interior", 559mm x 415mm.

37. R.E. Peterson and G.A. Newby, *"An Unreflected U^{235} Critical Assembly,"* Nucl. Sci. & Eng., **1** (May 1956) 112.

This work was performed under the auspices of the U.S. Department of Energy by Lawrence Livermore National Laboratory under contract No. W-7405-Eng-48.